A molecular representation of the potential of carbon monoxide adsorbed on a nickel surface

1989 J. Phys.: Condens. Matter 1 1551

(http://iopscience.iop.org/0953-8984/1/9/001)

J. Phys.: Condens. Matter **1** (1989) 1551–1559. Printed in the UK

A molecular representation of the potential of carbon monoxide adsorbed on a nickel surface

H C Poon and D K Saldin†
The Blackett Laboratory, Imperial College, Prince Consort Road, London SW7 2BZ, UK

Received 24 March 1988

Abstract. In a calculation of low-energy electron diffraction intensities from c(2 × 2) CO/Ni(100) we have considered a model of the potential of the adsorbate that preserves its molecular integrity. This representation of atomic muffin tins embedded in an interstitial potential bounded by an outer sphere mimics the model used in self-consistent-field Xα calculations for molecules. This enables us to determine some of the parameters of such a potential by comparison with experiment. Confirmation of the model is found in x-ray absorption near-edge structure.

1. Introduction

Amongst molecular absorbate systems, that of carbon monoxide on transition-metal surfaces has been one of the most widely studied. According to Blyholder's model [1], the charge transfer from occupied orbitals of the CO molecule to the $2\pi^*$ orbital above the Fermi level is mediated by the transition-metal substrate. It leads to a weakening of the CO σ-bond and is generally regarded as the crucial step in CO hydrogenation in Fischer–Tropsch synthesis. Apart from its importance in the understanding of the catalytic effect of transition-metal surfaces, it is also a stepping stone for the investigation of more complex molecular absorbate systems.

Low-energy electron diffraction (LEED) [2, 3] has proved to be one of the most successful of the surface spectoscopic probes in providing quantitative information about metal and semiconductor surfaces and those covered by atomic absorbates [4]. On the other hand, relatively few LEED studies have been conducted on molecular absorbate systems. In the case of CO, this is due partly to the experimental difficulties involved in monitoring the damage induced by the electron beam and the temperature-induced disorder. As a matter of fact, experiments on c(2 × 2)CO/Ni(100) have been done by three different groups [5–7], with measurements of the intensities of different sets of beams and over different energy ranges. Major differences are found in the regions of overlap. The only significant agreement is that between the intensities of the $(\frac{1}{2}\,\frac{1}{2})$ beam measured by Heinz and co-workers [7] and those of Passler and co-workers [6] in the energy range 50 to 120 eV. This is the only intensity/voltage (I/V) curve that shows many distinct features and extends over a wide energy range. This is also the only one used by Heinz and co-workers [7] for their structural analysis using the Zanazzi-Jona

† Present address: Department of Physics, University of Wisconsin–Milwaukee, PO Box 413, Milwaukee, WI 53201, USA.

0953-8984/89/091551 + 09 $02.50

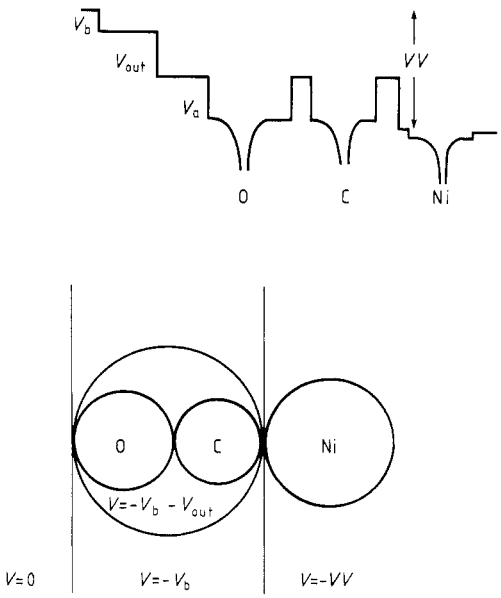

Figure 1. The model potential for CO/Ni(100).

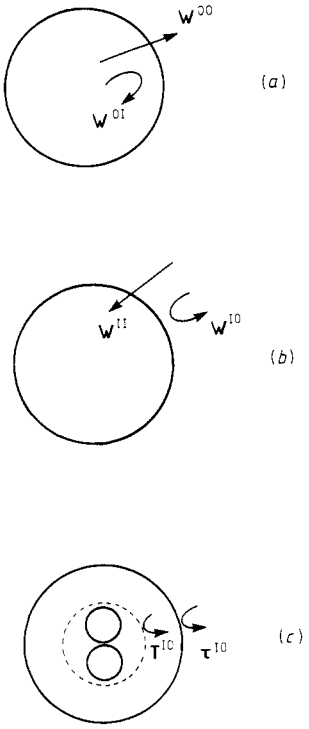

Figure 2. Scattering matrices for an electron incident on a spherical well from (*a*) the inside, (*b*) the outside. (*c*) An illustration of the relation between the bare 'in–out' scattering matrix $\mathbf{T}^{IO}$ of the molecule and that $\boldsymbol{\tau}^{IO}$ after correction for the outer-sphere discontinuity.

reliability (*R*) factor [8]. On the theoretical side, the situation is also less than satisfactory [5–7, 9]. To date only Andersson and Pendry [5] have published in *R*-factor analysis for the CO/Ni(100) and CO/Cu(100) systems with an extensive beam set. It is the aim of this paper to investigate the effect of a more realistic model of the molecular potential and to determine some of its parameters by comparison with experimental LEED data. Additional evidence from x-ray absorption near-edge structure (XANES) is also considered.

2. Potentials and phase shifts

A problem with the muffin-tin representation of the atomic potentials in a CO molecule is the contrast between the very deep potential between the carbon and oxygen atoms and the relatively weak potential in the exterior of the molecule. This contrast frequently gives rise to unphysically large discontinuities at the atomic muffin-tin radii even in self-consistent electronic structure calculations. The problem can be alleviated to some extent by the inclusion of a spherical outer sphere surrounding the molecule, of constant potential outside the atomic muffin tins and a discontinuity in the potential at the boundary of the outer sphere (figure 1). A self-consistent electronic structure calculation

for such a model potential would be expected to yield reduced discontinuities at the atomic muffin-tin radii with a finite one at the outer-sphere boundary. It is of interest to investigate whether there is any experimental justification for such a model.

Accordingly we re-analysed the experimental LEED data [5–7] for CO/Ni(100) in the light of this model for the CO potential and attempted to determine empirically the values of the atomic, V_a, and outer-sphere, V_{out}, potential discontinuities. We began with the O and C muffin-tin potentials from an O–C–Ni multiple-scattering Xα cluster calculation [9] which generates large discontinuities, $V_a = 65$ eV, at the atomic muffin-tin radii and a smaller one at the boundary of the three-atom cluster. We used the same inner muffin-tin potentials, but treated V_a and V_{out} as parameters to be optimised by the LEED data. The inner potential in the Ni substrate was taken to be -11.2 eV while that, V_b, in the CO overlayer was tuned after V_a and V_{out} had been fixed at their optimised values. The Ni muffin-tin potential used was that obtained from a conventional band-structure calculation [10]. The C and O phase shifts were recalculated in the standard manner [2] (by outward integration of the radial Schrödinger equation) for each different discontinuity V_a of the atomic potential.

3. Electron scattering by the CO overlayer

We follow the 'molecular-atom' approach of Andersson and Pendry [5] in treating the CO overlayer. The CO molecule is regarded as a unit in respect of its scattering properties and we define a molecular scattering matrix $\mathbf{T}^{IO}$, whose elements relate the amplitudes A^0_{lm} of a set of incoming spherical waves $j_l(\kappa|\boldsymbol{r} - \boldsymbol{R}_0|)Y_{lm}(\boldsymbol{r} - \boldsymbol{R}_0)$ to those, $A^{(s)}_{LM}$, of a set of outgoing spherical waves $h^{(1)}_L(\kappa|\boldsymbol{r} - \boldsymbol{R}_0|)Y_{LM}(\boldsymbol{r} - \boldsymbol{R}_0)$, where

$$A^{(s)}_{LM} = \sum_{lm} A^{(0)}_{lm} T^{IO}_{lm,LM}. \tag{1}$$

$\boldsymbol{\kappa}$ is the wavevector, l, m, L, M are angular momentum quantum numbers and j_l and $h^{(1)}_l$ are lth-order spherical Bessel and Hankel functions.

The matrix $\mathbf{T}^{IO}$ is related to the elements

$$t_{jl} = [\exp(2i\delta_{jl}) - 1]/2 \tag{2}$$

of the t-matrix of the jth atom (where δ_{jl} represents its phase shift of quantum number l) and to the propagators $G_{l'm',l''m''}(\boldsymbol{R}_j - \boldsymbol{R}_0)$, which re-expand the spherical wave amplitudes about the positions $\boldsymbol{R}_j$ of the individual atoms of the molecule.

We use some routines borrowed from a program [11, 12] that computes XANES to calculate the matrix $\mathbf{T}^{IO}$. In the presence of an 'outer-sphere' potential discontinuity surrounding the molecule, this 'bare' scattering matrix needs to be modified by the scattering properties of the outer sphere.

The latter are calculated as follows. Consider an outgoing electron wave incident on the outer sphere (of radius a) from the inside (see figure 2(a)). The boundary conditions for the continuity of the wavefunction and its derivative with respect to the radial coordinate (denoted by the primes in equations (4) to (11)) give rise to the following equations:

$$Ah^{(1)}_l(\eta) + Bj_l(\eta) = Ch^{(1)}_l(\varepsilon) \tag{3}$$

$$Ah_l^{(1)'}(\eta) + Bj_l'(\eta) = C(\varepsilon/\eta)h_l^{(1)'}(\varepsilon) \tag{4}$$

where $\varepsilon = ka$, and $\eta = Ka$, with $k = \sqrt{2(E - V_{\text{out}})}$, and $K = \sqrt{2E}$, and E is the electron's energy.

Hence we find the elements of the 'out–out' and 'out–in' scattering matrices W_l^{OO} and W_l^{OI}, of the outer-sphere boundary to be given by

$$W_l^{\text{OO}} = C/A = (j_l(\eta)h_l^{(1)'}(\eta) - h_l^{(1)}(\eta)j_l'(\eta))/D_l \tag{5}$$

$$W_l^{\text{OI}} = B/A = [h_l^{(1)}(\varepsilon)h_l^{(1)'}(\eta) - (\varepsilon/\eta)h_l^{(1)}(\eta)h_l^{(1)'}(\varepsilon)]/D_l \tag{6}$$

where

$$D_l = (\varepsilon/\eta)j_l(\eta)h_l^{(1)'}(\varepsilon) - h_l^{(1)}(\varepsilon)j_l'(\eta). \tag{7}$$

Next, consider a spherical wave incident from the outside on the outer-sphere boundary (see figure 2(*b*)). The boundary conditions yield:

$$Aj_l(\varepsilon) + Bh_l^{(1)}(\varepsilon) = Cj_l(\eta) \tag{8}$$

$$Aj_l'(\varepsilon) + Bh_l^{(1)'}(\varepsilon) = C(\eta/\varepsilon)j_l'(\eta) \tag{9}$$

from which the elements W_l^{II} and W_l^{IO} of the 'in–in' and 'in–out' scattering matrices of the outer sphere are found to be:

$$W_l^{\text{II}} = C/A = (j_l(\varepsilon)h_l^{(1)'}(\varepsilon) - h_l^{(1)}(\varepsilon)j_l'(\varepsilon))/D_l \tag{10}$$

$$W_l^{\text{IO}} = B/A = [j_l(\varepsilon)j_l'(\eta) - (\varepsilon/\eta)j_l(\eta)j_l'(\varepsilon)]/D_l. \tag{11}$$

If $\boldsymbol{\tau}^{\text{IO}}$ represents the 'in–out' scattering matrix of the molecule in the presence of the outer-sphere potential, we may deduce (see figure 2(*c*)) that

$$\boldsymbol{\tau}^{\text{IO}} = \mathbf{W}^{\text{IO}}(\mathbf{1} - \mathbf{T}^{\text{IO}}\mathbf{W}^{\text{OI}})^{-1}\mathbf{T}^{\text{IO}}\mathbf{W}^{\text{OO}} + \mathbf{W}^{\text{IO}}. \tag{12}$$

Using the matrix $\boldsymbol{\tau}^{\text{IO}}$ it is possible to construct the elements

$$M_{g'g}^{\pm\pm} = \frac{8\pi^2}{|k_0^{\pm}|Ak_{gz}^{+}} \sum_{LL'L'} \mathrm{i}^{l-l'}\, Y_L^*(\boldsymbol{k}_g^{\pm})(\mathbf{1} - \mathbf{X})_{LL''}^{-1}\, \tau_{L''L'}^{\text{IO}} Y_{L'}(\boldsymbol{k}_{g'}^{\pm}) \tag{13}$$

of a standard LEED reflection matrix [2, 3] for an ordered layer relating the amplitude of a plane wave of wavevector $\boldsymbol{k}_g^{\pm}$ incident on the layer to one of wavevector $\boldsymbol{k}_{g'}^{\pm}$ emerging from it. The factor $(\mathbf{1} - \mathbf{X})^{-1}$ takes account of the multiple scattering within the layer, A is the area of the surface unit cell and the subscript z refers to the component normal to the surface.

The reflection matrix of the Ni substrate was calculated using the layer-doubling algorithm [2, 3] and the reflection matrix of the combined adsorbate–substrate system found by the standard methods involving matrix inversion [2, 3]. By this means, the LEED intensities from CO adsorbates on transition-metal surfaces were calculated.

4. Determination of the potential parameters

We optimise our potential parameters V_{b}, V_{a} and V_{out} of CO molecules adsorbed as a c(2 × 2) overlayer on a Ni(100) substrate by monitoring the agreement between our calculations and experimental LEED intensities using the reliability factor introduced by Pendry [13]. The geometrical parameters were fixed at the values determined by

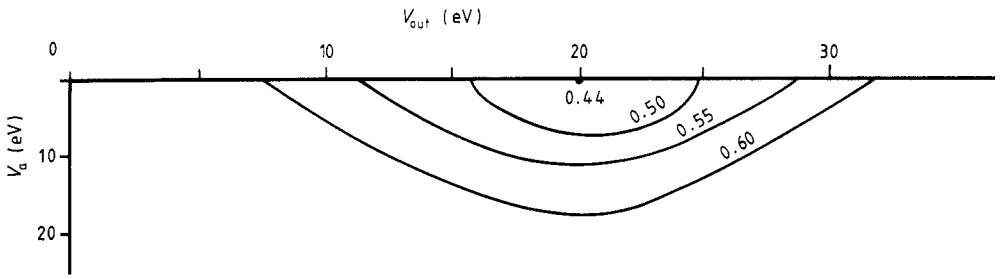

Figure 3. A contour map of the Pendry R-factor for the $(\frac{1}{2}\frac{1}{2})$ beam of the experiment of [7] on c(2 × 2)CO/Ni(100) plotted with respect to V_a and V_{out}.

Andersson and Pendry [5]—that is, the CO molecules were assumed perpendicular to the surface and adsorbed on the atop sites, with O–C bond lengths of 1.15 Å and C–Ni distances of 1.71 Å.

4.1. Analysis of the data of Heinz and co-workers [7]

The contour map of the Pendry R-factor for $V_b = 0$ is plotted with respect to V_a and V_{out} in figure 3. Only the $(\frac{1}{2}\frac{1}{2})$ beam of the experiment was used. The integral-order-beam I/V curves are dominated by substrate scattering as seen from its similarity to the I/V curves for pure Ni(100) [7]. On the other hand, since half-order beams are present only in the presence of an overlayer, we expect them to be sensitive to the overlayer potential. As the $(\frac{1}{2}\frac{1}{2})$ is the only half-order beam in the experiment, we have used only this beam for the R-factor analysis. The minimum is located at about $V_{out} = 20$ eV and $V_a = 0$ eV. The minimum R-factor was found to be 0.44. The implication is that this experiment favours a discontinuity of 20 eV at the outer-sphere boundary, while the atomic potential joins smoothly to the interstitial region inside the outer sphere.

Keeping $V_{out} = 20$ eV and $V_a = 0$, the surface barrier V_b was varied. We found that the R-factor minimum moved to $V_b = 3$ eV with a value of 0.38. Thus in addition to an outer-sphere discontinuity of 20 eV, a small barrier of 3 eV was favoured. The experimental and theoretical I/V curves for these optimised parameters are shown in figure 4.

4.2. Analysis of the data of Andersson and Pendry [5]

We repeated the analysis in § 4.1, for the (1 0), (1 1), $(\frac{1}{2}\frac{1}{2})$ and $(\frac{1}{2}\frac{3}{2})$ beams of the experiment. The corresponding contour map is shown in figure 5. Once again a zero discontinuity at the atomic boundary was favoured, although the minimum was now located at $V_{out} = 12$ eV.

When the surface barrier V_b was varied, it was found that the minimum remained at $V_b = 0$. The corresponding experimental and theoretical I/V curves are shown in figure 6.

5. XANES and the band structure for CO/Ni(100)

Studies of XANES by Stohr and Jaeger [14] on CO/Ni(100) for O 1s and C 1s excitations indicate that the molecular orbitals of CO persist even when the molecule is adsorbed

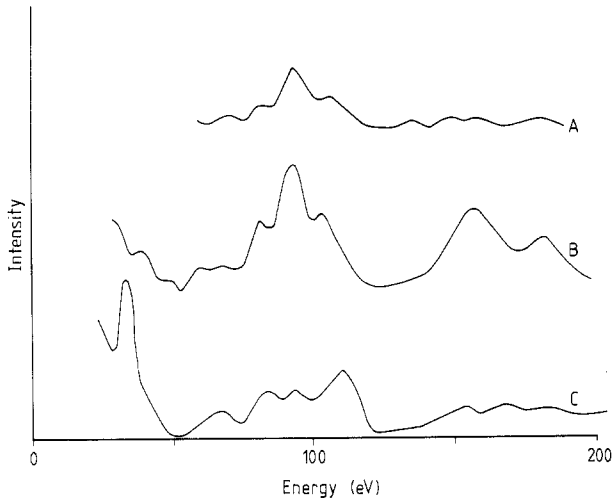

Figure 4. Experimental I/V plots for the $(\frac{1}{2}\,\frac{1}{2})$ beams from (A) [6] and (B) [7] for c(2 × 2) CO/Ni(100) and (C) corresponding optimised theoretical results with $V_b = 3$ eV, $V_{out} = 20$ eV and $V_a = 0$.

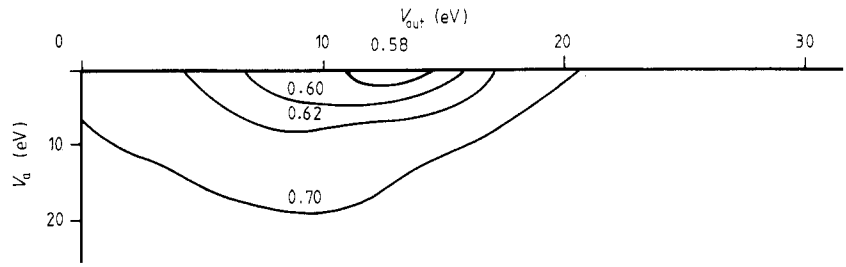

Figure 5. As figure 3, but for the data from [5] with an average taken over the (10), (11), $(\frac{1}{2}\,\frac{1}{2})$ and $(\frac{1}{2}\,\frac{3}{2})$ beams.

on Ni. Employing the C, O and Ni potentials used in the LEED calculation, we have confirmed by a band-structure calculation [15] that, although there occurs considerable charge transfer between the CO and the Ni substrate, the molecular resonances can still be identified.

Another and more direct way of assessing the model potential used in the previous section would be to compare a calculation of XANES with the experimental observations. The XANES intensity for an isolated molecule is just its total photoemission cross section. It is given by [11]

$$W = -2\langle i|\Delta^+ \operatorname{Im} G^+ \Delta|i\rangle \tag{14}$$

where $|i\rangle$ represents the initial core state, G^+ the Green function of the excited electron and $\Delta = -\mathrm{i}\boldsymbol{A}\cdot\boldsymbol{\nabla}/c$ the electron–photon interaction.

The electromagnetic interaction giving rise to the transitions imposes very specific selection rules relating the angular momentum quantum numbers of the initial and final states. Thus for the excitation of an atomic K-shell the dipole selection rule $\Delta l = \pm 1$ implies that the excited electrons must be characterised by angular momentum quantum

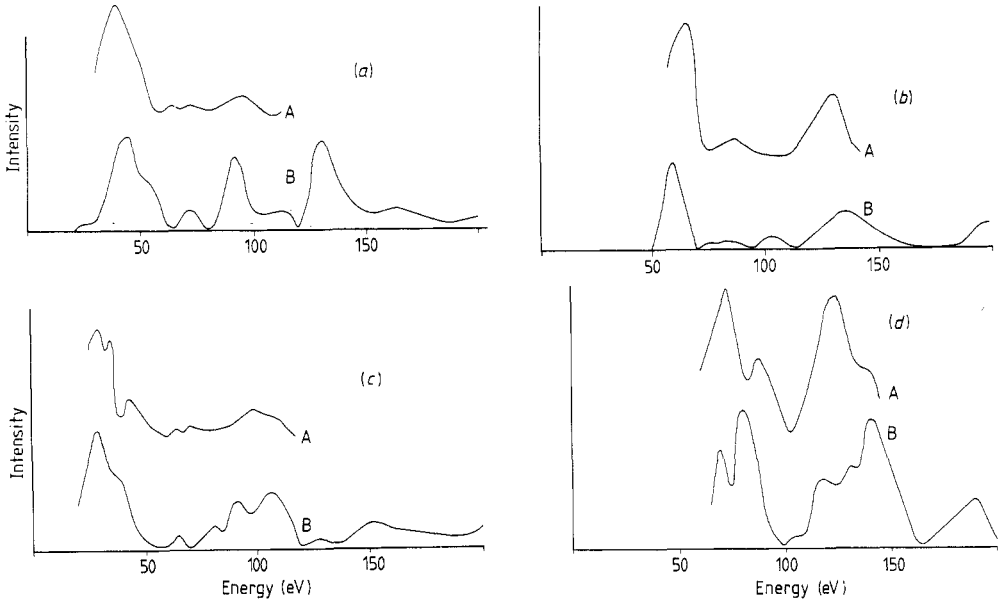

Figure 6. Andersson and Pendry's experimental [5] I/V plots (A) for c(2 × 2)CO/Ni(100) and corresponding optimised theoretical results (B) with $V_b = 0$, $V_{out} = 12$ eV and $V_{in} = 0$. (*a*) (10) beam, (*b*) (11) beam, (*c*) $(\frac{1}{2}\,\frac{1}{2})$ beam, (*d*) $(\frac{1}{2}\,\frac{3}{2})$ beam.

number $l = 1$. The polarisation of the exciting radiation similarly imposes selection rules on the azimuthal quantum number m. Taking the polar axis along the axis of the CO molecule, if $\boldsymbol{A}$ is directed parallel to this axis, electrons are excited into orbitals characterised by $m = 0$, and if $\boldsymbol{A}$ is perpendicular to this axis, the electrons are ejected into orbitals characterised by $m = \pm 1$, for the same K-shell excitations (for which of course $m = 0$). If we insert complete sets of final states $|f\rangle$ in (14) above, it can be re-expressed as:

$$W = -2\langle i|\Delta^+|f\rangle\langle f|\operatorname{Im} G^+|f\rangle\langle f|\Delta|i\rangle \tag{15}$$

or

$$W = 2\pi\rho_f|M| \tag{16}$$

where

$$\rho_f = -\langle f|\operatorname{Im} G^+|f\rangle/\pi \tag{17}$$

is the density of states projected onto the final state $|f\rangle$ and

$$M = \langle f|\Delta|i\rangle \tag{18}$$

is the matrix element for the transition. Thus the XANES intensity is essentially a measure of the density of final states coupled to by the atomic transition, modulated by a slowly varying matrix element M.

It follows that the polarisation dependence of the XANES intensity can be exploited to probe molecular electronic structure. In the case of CO/Ni the back-scattering of the ejected core electrons from the environment is small and we have calculated the XANES by considering only the isolated molecule.

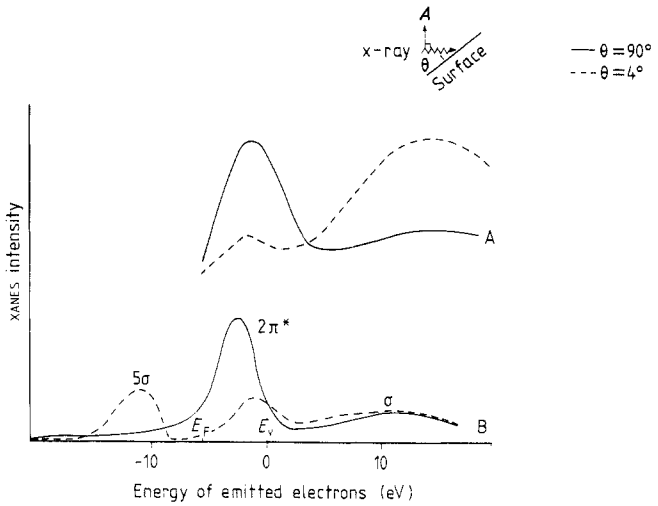

Figure 7. Experimental (A) and theoretical (B) XANES intensity from oxygen 1s excitations for CO/Ni(100). The vectors A of the photon beam were inclined at $\theta = 4°$ and 90·° to the surface normal. The calculations were based on the model potential deduced from the LEED data from [7] with $V_b = 3$ eV, $V_{out} = 20$ eV and $V_a = 0$. E_F and E_v represent the Fermi and vacuum levels respectively.

Figure 7 shows the calculated XANES distribution for the potential model favoured by the experiment of Heinz and co-workers [7]. From their peak positions and polarisation dependence, the 5σ, $2\pi^*$ and σ shape resonances above the vacuum can be clearly identified. Only the $2\pi^*$ and σ shape resonances above the Fermi level are observable in the XANES experiments [14] whose results are shown in the same figure. We have taken the work function to be 5.5 eV. A surface barrier of 3 eV, as determined from the LEED experiment of [7], is necessary here in order to have the $2\pi^*$ shape resonance lying below the vacuum.

The parameters of our model potential were derived from a fit to experimental LEED spectra at energies in the approximate range 25–200 eV. On the other hand, ejected atomic core electrons responsible for XANES have energies less than about 20 eV, and some caution may need to be exercised in extending the scope of our potential parameters to such energies. Indeed, the lack of a polarisation dependence in the theoretical calculations of the peak corresponding to the σ shape resonance may be some indication of the need for such reserve. Nevertheless, the energies of the $2\pi^*$ and σ shape resonances and the polarisation dependences of the 5σ and $2\pi^*$ peaks show good agreement between experiment and theory.

6. Conclusions

In analogy with molecular multiple-scattering Xα calculations, a model potential with an outer-sphere boundary has been introduced for a molecular absorbate on the surface of a metal. This model has been used in a LEED calculation, which has been compared with published experimental data for the system CO/Ni(100). An analysis of the data of [7] using the Pendry reliability factor indicated that the best agreement occurred for a

vacuum–overlayer surface barrier of about 3 eV and an outer-sphere potential of about 20 eV below this level. In the model that gave the optimum agreement, the atomic potentials were found to join smoothly to the interstitial region inside the sphere. Similar conclusions were found upon analysis of the data of [5], except that an outer-sphere discontinuity of 12 eV was favoured and no vacuum–overlayer surface barrier.

This contrasts with the model potential commonly used in LEED calculations, i.e. two potential steps (one between the vacuum and the molecular layer, another between the molecular layer and the substrate) and large discontinuities at atomic muffin-tin boundaries. Our model preserves the independence and integrity of the molecules and has the advantage that parameters determined by comparison with experiment may be compared directly with those from self-consistent-field $X\alpha$ layer calculations for the adsorbates [15].

Further evidence for the validity of the model is provided by its use in the interpretation of XANES from the same adsorbate system.

Acknowledgments

The authors wish to thank Professor J B Pendry FRS for suggesting the work described, and for many helpful discussions.

References

[1] Blyholder G 1964 *J. Phys. Chem.* **68** 2772
[2] Pendry J B 1974 *Low Energy Electron Diffraction* (London: Academic)
[3] Van Hove M A and Tong S Y 1978 *Surface Crystallography by LEED* (New York: Springer)
[4] Maclaren J M, Pendry J B, Rous P J, Saldin D K, Somorjaio G A, Van Hove M A and Vvedensky D D 1987 *Surface Crystallographic Information Service* (Dordrecht: Reidel)
[5] Andersson S and Pendry J B 1980 *J. Phys. C: Solid State Phys.* **13** 3547
[6] Passler M, Ignatiev A, Jona F, Jensen P W and Marcus P M 1979 *Phys. Rev. Lett.* **43** 360
[7] Heinz K, Lang E and Muller K 1979 *Surf. Sci.* **87** 595
[8] Zanazzi E and Jona F 1977 *Surf. Sci.* **62** 61
[9] Tong S Y, Maldonado A, Li C H and Van Hove M A 1980 *Surf. Sci.* **94** 73
[10] Wakoh S 1965 *J. Phys. Soc. Japan* **20** 1894
[11] Durham P J, Pendry J B and Hodges C H 1982 *Comput. Phys. Commun.* **25** 193
[12] Vvedensky D D, Saldin D K and Pendry J B 1986 *Comput. Phys. Commun.* **40** 421
[13] Pendry J B 1980 *J. Phys. C: Solid State Phys.* **13** 937
[14] Stohr J and Jaeger R 1982 *Phys. Rev.* B **26** 4111
[15] Poon H C 1989 *J. Phys.: Condens. Matter* submitted